EUROfusion

EUROFUSION WPS1–PR(15)06

A. Rodatos et al.

Detecting Divertor Damage During Steady State Operation of W7–X

Preprint of Paper to be submitted for publication in
Review of Scientific Instruments

This work has been carried out within the framework of the EUROfusion Consortium and has received funding from the Euratom research and training programme 2014-2018 under grant agreement No 633053. The views and opinions expressed herein do not necessarily reflect those of the European Commission.

Detecting divertor damage during steady state operation of W7-X

A. Rodatos,[1, a)] J. Boscary,[2] H. Greuner,[2] M. W. Jakubowski,[1] R. König,[1] T. S. Pedersen,[1] and G. A. Wurden[3]

[1)] *Max Planck Institute for Plasma Physics, Wendelsteinstr. 1, Greifswald, Germany*

[2)] *Max Planck Institute for Plasma Physics, Boltzmannstr. 2, Garching, Germany*

[3)] *Los Alamos National Laboratory, Los Alamos, NM 87544 USA*

(Dated: April 29, 2015)

Wendelstein 7-X aims to demonstrate the reactor capability of the stellarator concept, by creating plasmas with pulse lengths of up to 30 minutes at a heating power of up to 10 MW. The divertor plasma facing components will see convective steady state heat flux densities of up to $10\,MW/m^2$. These high heat flux target elements are actively cooled and are coverd with CFC as plasma facing material. The CFC is bonded to the CuCrZr cooling structure. Over the life-time of the experiment this interface may weaken and cracks can occur, greatly reducing the heat conduction between the CFC tile and the cooling structure. Therefore, there is not only the need to monitor the divertor to prevent damage by overheating, but also the need to detect these fatigue failures of the interface. A method is presented for an early detection of fatigue failures of the interface layer, solely by using the information delivered by the IR-cameras monitoring the divertor. This was developed and validated through experiments made with high heat flux target elements prior to installation in-to W7-X.

[a)] Electronic mail: Alexander.Rodatos@ipp.mpg.de

I. INTRODUCTION

Wendelstein 7-X (W7-X), an optimized modular stellarator, will be one of the very first experiments that will generate quasi-steady-state plasmas with fusion relevant parameters. The device will have discharge durations of up to 30 minutes and continuous injected power of up to 10 MW. One of the major challenges for this experiment is a reliable and continuous operation to demonstrate the reactor capability of the stellarator concept. The plasma facing components (PFCs), especially the highly heat loaded *divertor*, responsible for particle and power exhaust, need to be monitored for operating the experiment safely. W7-X is designed with low Z (low atomic number) PFCs to reduce the plasma radiation due to impurities.

Figure 1: Example of a prototype of the W7-X divertor target element. It consists of 10 CFC tiles (with a thickness of 8 mm, a length of ≈ 25 mm and a width of ≈ 55 mm) bonded by copper inter-layers to a water-cooled CuCrZr heat sink. The numbers indicated on the tile surfaces denote thickness of the a-C:H surface layers used to emulate real surface layers building up during the W7-X operation.

Consistent with the five fold symmetry of the magnetic configuration, the experiment is divided into five nearly identical parts[27]. Each of these modules contains two divertor units and each unit is composed of different areas, capable of dissipating different heat flux densities (further called heat flux) depending on the expected loading. The largest is the so-called high heat flux (HHF) target area, designed for steady-state heat fluxes of up to 10 MW/m^2. The HHF target area is built from 10 target modules, each of which in turn consists of 8 to 12 target elements. These target elements are of different types, which are 250 mm to 600 mm long and have a width of 50 mm to 61.5 mm. On the plasma-facing side they are covered with about 16000 tiles, 8 mm thick, made from carbon fibre reinforced carbon (CFC). In the Case of W7-X CFC NB-31 is used[42]. Before installation of the divertor targets in to the machine the surface will be 3D-machined reducing the tile thickness up to 3 mm. The cooling structures of these elements are water cooled CuCrZr heat sink[24](See Figure 1). Due to different thermal expansion coefficients of Cu and CFC, a compliant layer

is needed as an interface. Experience with similar technology from Tore Supra showed that the compliant layer has a limited lifetime and cracks will start to form over time[40]. Therefore this technology was further developed for use at W7-X by introducing an additional layer of soft Cu to lessen the thermomechanical stress in the compliant layer. For heat fluxes below $8\,MW/m^2$ no crack propagation was observed while for higher heat fluxes the crack propagation was strongly reduced in comparison to early designs of the interface layer[30].
We name the interfaces showing these cracks *delaminated*; they show strongly reduced heat conductivity between the CFC tile and the heat sink. At the tile edges these defects appear as macroscopic cracks in the interface layer and can be detected by visual inspection[23]. Under heat load, delaminated areas will show elevated surface temperatures and the thermomechanical stress induced by high heat loads (e.g. at $q_{\mathrm{surf}} > 8$ MW/m^2), may cause a propagation of the delaminated interface area with every further heat cycle[30].W7-X is equipped with an in-vessel set of control coils allowing one to manipulate the strike line position and by that preventing excessive heat loads on delaminated tiles. A prerequisite to avoid further growth of the delaminated area by moving the strike line away is to identify those defects, before they reach sizes which could compromise safe operation. Therefore, in order to avoid such failures, a divertor surveillance system is under development at W7-X, whose central hardware components are 10 endoscope systems using infrared cameras operating in the wavelength range of $3\,\mu m$ to $5\,\mu m$. Each endoscope system is designed to observe the entire divertor with a spatial resolution of 6 mm to 10 mm on the divertor surface[25,37,38]. For a typical CFC tile size of 25 x 50 mm this is barely enough to resolve its surface temperature.
This work focuses on developing robust and reliable criteria for safe-guarding and diagnosing the divertor in real-time using the infrared security system described above. First, in Section II, a heuristic model is used to illustrate the behaviour of an intact and delaminated tile under varying heat load. Additionally we discuss so-called surface layers formed on a tile surface during experiments. The heuristic description is used to present reasons to use more sophisticated analysis than a simple threshold surface temperature. In Section III our approach is quantified by introducing a finite element model for heat transport inside intact and delaminated tiles. In Section IV we analyze experimental data and develop the criteria to distinguish between intact and defective tiles. One of the major challenges using infrared surveillance of PFCs in magnetic fusion devices with carbon as plasma-facing

material (PFM) comes from the formation of so-called *surface layers*. In W7-X we expect mostly soft and hard amorphous carbon-hydrogen compounds (a-C:H) forming those layers. In Section V we test if the developed criteria work in the presence of artificially introduced surface layers. Finally, the conclusions are presented in Section VI.

II. HEURISTIC DESCRIPTION OF INFRARED THERMOGRAPHY IN THE PRESENCE OF DELAMINATIONS AND SURFACE LAYERS

Experience from other fusion experiments shows that the observed infrared emission from a PFC does not unambiguously allow a determination whether a very high infrared emission rate is caused by an unusually large incident heat load, the presence of a poorly bonded a-C-H surface layer, or a partially or fully delaminated tile. The problem is sketched out in a cartoon fashion in Figure 3. The three parts of the Figure shown represent the three basic cases that are of particular interest to us for the divertor in W7-X:

- an intact, virgin tile with a good contact to the underlying cooling structures
- a delaminated tile, a tile for which a smaller or larger part of the CFC has been disconnected from the cooling structure due to one or several cracks
- a tile with a so-called *surface layer*. Such layers can appear on both intact and delaminated tiles.

The appearance of surface layers has been reported in many fusion devices e.g. ASDEX Upgrade[36], W7-AS[34], JET[22] or Tore Supra[39]).

Poorly thermally bonded surface layers with thicknesses from 1 to a few hundred μm are often observed in "carbon" faced experiments[39], and these are particularly troublesome for thermography, since they heat up to very high temperatures even at rather low heat fluxes, and therefore are at risk of causing false alerts for a safety interlock system of the divertor.

In a fusion experiment, the local heat loads onto the PFCs are not known in detail a priori, due to rather complicated interaction between plasma heating, transport and magnetic equilibrium. While the total heat transported to the divertor in steady state is limited by

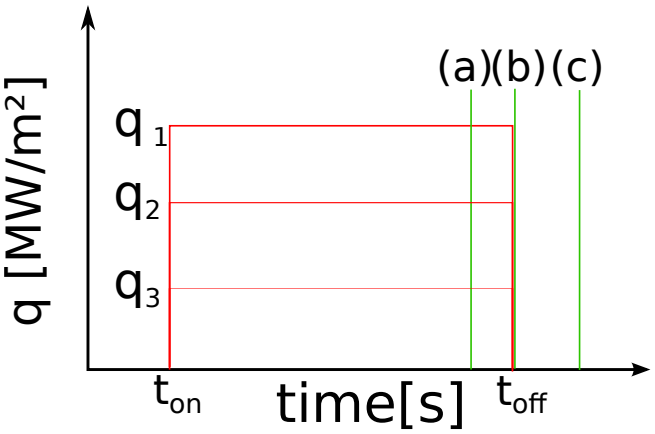

Figure 2: Heat load scenario discussed in Sec. II. The abscissa shows heat flux density q onto a plasma facing component as a function of time (the ordinate).q_1 to q_3 show the corresponding heat flux densities for the three cases (I to III) shown in figure 3.

the plasma heating, and/or fusion power released by α-particles, the distribution of the heat load is determined by the edge magnetic topology and heat transport processes. Generally, areas with a high heat flux density are adjacent to areas with much lower heat fluxes. If the thermal properties of the divertor target elements are known in detail, the heat flux can be deduced from the steady state surface temperature in a rather straightforward way. In reality, however, the thermal properties of the surface change during the operation and a mixture of the cases presented in Figure 3 will occur over the target tiles lifetime. This makes calculations of heat fluxes nontrivial and presents a challenge for a safety-interlock system. In Figure 2 the heat load scenario for the discussed cases is shown. Each tile is exposed to a spatially uniform heat load during the time from t_{on} until t_{off}. The power is turned on and off with a rise and a decay time much shorter than PFCs' characteristic time for a heat pulse propagation. The three tiles receive vastly different heat loads, but all have an identical surface temperature. The temporal behavior shows marked differences though. Depending on the time period at which we would observe a given PFC we would see different behaviour of an intact virgin tile (I - left column in Figure 3), a delaminated tile (II - middle column in Figure 3) and an intact tile with a surface layer on top (III - right column in Figure 3).

(a): After some time of exposure to constant heat flux, the target tile reaches a thermal equilibrium and therefore a constant surface temperature. The heat is mainly removed from the

CFC-tile by thermal conduction to the heat sink. At surface temperatures of '1000 $°C$ (which is the expected surface temperature of an intact divertor tile under a heat load of 10 MW/m^2) heat transport by radiation from the surface of the CFC tile to the surroundings can be neglected. The radiated power from the CFC-tile is blackbody radiation, $p \propto \sigma_{SB} T^4$, with σ_{SB} being Stefan-Boltzmann's constant. Heat conduction will be the dominant heat transport mechanism for case I and II. In the presence of a surface layer (case III) however the radiation losses cannot be neglected. Due to the low heat capacity of the thin surface layer, its poor thermal contact, and the strongly non-linear temperature dependence of blackbody radiation, high surface temperatures will be reached quickly, even for relatively low heat loads. Depending on the thermal properties of the layer and how well it is thermally connected to the bulk material the surface temperature can be several hundred Kelvin higher if a layer is present. During the steady-state phase where the temperature does not change, one cannot determine whether a local high surface temperature is caused by delamination, surface layers, or an unexpectedly high incident heat load.

(b): At $t = t_{\text{off}}$, the heating stops. In a fusion experiment this can happen by moving away a strike line from a target element or by stopping the plasma heating (in this case the energy confinement time needs to be taken in to account). During the first few hundred milliseconds after t_{off}, an initially hot tile covered by a co-deposited surface layer will show a very fast surface temperature decay, since the heat capacity is so low. Despite the low thermal connectivity, a new thermal equilibrium between the surface layer and the CFC tile is reached, and the temperature of the surface layer matches the temperature of the underlying CFC tile. In the same phase, intact tiles as well as un-coated delaminated tiles show slower temperature decays since their thermal capacities are much larger than for a surface layer and any thermal conduction occurs on slower time scales. Since the intact tile has better thermal transport than the delaminated tile, the delaminated tile cools off slower than the intact tile (case I and case II in Fig. 3(b)) but not necessarily slow enough to be detectable.

(c): At $\approx 7\,\text{s}$ after t_{off} the tile with no defect reaches a new thermal equilibrium with a constant surface temperature equal to the temperature of the coolant. On the other hand, the delaminated tile will still

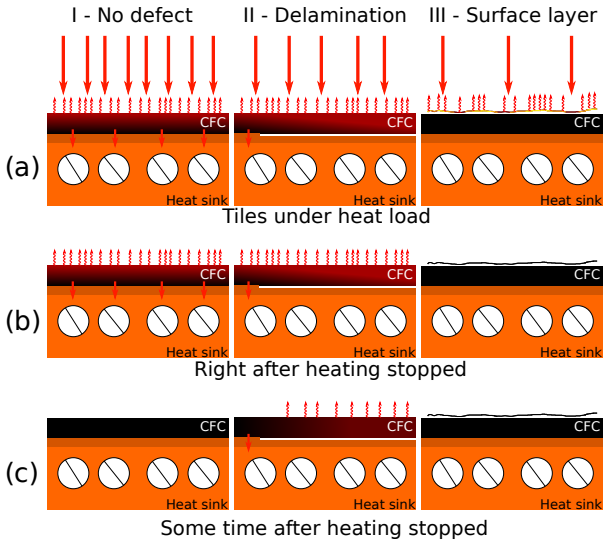

Figure 3: Sketched behaviour of the surface temperature after the heat flux to the surface was stopped. intact (left), delaminated(center) and a coated (right) tile. In case II the heat removal capacity is reduced because of the damaged interface. Heat removal is only possible over the part of the interface that is still intact.

show an elevated surface temperature, since the heat conduction through the CFC is anisotropic: The target elements for W7-X are constructed in such a way that heat conduction from the plasma facing surface towards the heat sink(vertical) is much stronger than perpendicular to this direction. The minimum specification for thermal conductivity at $800\,^{\circ}C$ is $125\,Wm^{-1}K^{-1}$ vertical and $50\,Wm^{-1}K^{-1}$ horizontal[42].

III. FEM CALCULATIONS

The calculations using the finite element method (FEM) were performed with ANSYS using a model of the high heat flux targets[41]. Since heat loads up to $10\,MW/m^2$ are expected , this value was used in the calculations, with a pulse duration of 10 s. The heat flux was distributed uniformly over the target surface. In order to simplify the calculations, only two mechanisms of cooling were considered: conductive transport from the tile surface towards the cooling channels and radiation losses from its surface. The model of the target element was adapted to include delamination defects and surface layers. In order to represent delaminated areas in the ANSYS code, the thermal connection between CFC material and the heat sink was removed. Delaminated areas of different size were simulated, in order to study the influence of defect size on the cooling behaviour. In order to represent the

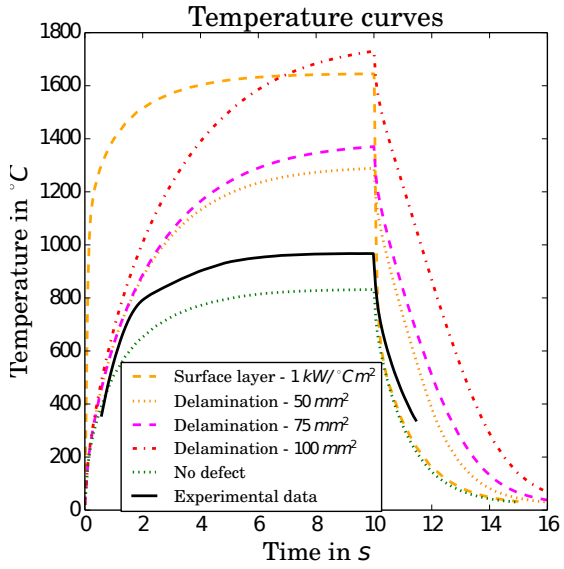

Figure 4: Surface temperature curves for tiles of different status. Data was gained by FEM calculations. Heating was switched off at $t_{off} = 10\,\mathrm{s}$. The different transient behaviour for target tiles with a surface layer, delamination or intact described in section II are visible. The experiment from which the experimental data (continues line) is taken is described in section V. The experimental temperature curves represents a case with no surface layer and no delamination.

surface layer in the model, a thin layer (thickness of 0.1 mm) with a heat transfer coefficient of $10\,kW/Km^2$ was added at top of the tile. The mesh size is 1 mm for the CFC-Tile and 2 mm for the heat sink. Figure 4 shows the transient surface temperature, for all the cases. We have found that the different transient behaviour can be well characterized by a temperature decay time τ[40], defined as:

$$\tau = \frac{T}{\frac{dT}{dt}} = \frac{T(t_i)}{\frac{T(t_i)-T(t_{i+1})}{t_i - t_{i+1}}}. \tag{1}$$

τ allows us to get the characteristic time scale for the cooling process independent of the absolute temperature. Figure 5 shows the evolution of τ for all the discussed cases. After the heating is stopped, ($t_{off} = 10\,\mathrm{s}$) τ increases strongly. In the case of the intact tile and the tile with the surface layer, τ become constant afterwards, while in the case of delamination a maximum value is reached and after a short flat-top phase, τ begins to drop again. The height of the maximum increases with the size of the delaminated area. This is a result of the decreased overall heat transport from the tile to the heat sink for growing defect size. For comparing different cases $\tau(t = 10.5\,\mathrm{s})$ from the flat-top phase is used,

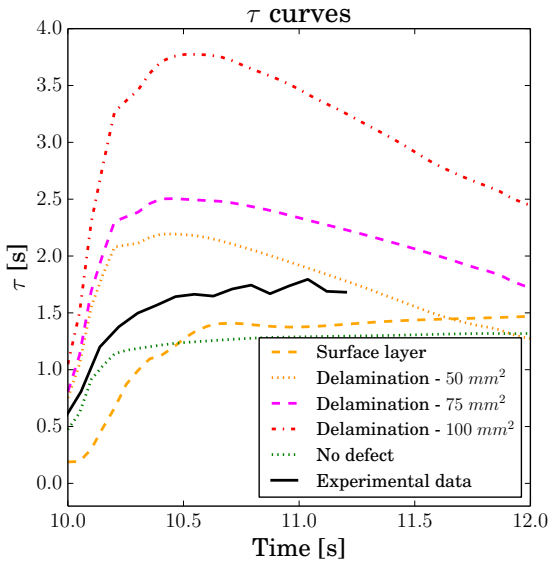

Figure 5: τ for the different cases. Beam off at $t_{off} = 10\,\mathrm{s}$. The different states of the CFC-tile are clearly distinguishable by the different behaviour for τ.

Table I: Values of $\tau(t = 10.5\,\mathrm{s})$ for the different cases shown in figure 5

Case	$\tau(t = 0.5\,\mathrm{s})[s]$
No defect	1.24
Delamination $50\,\mathrm{mm}^2$	2.19
Delamination $75\,\mathrm{mm}^2$	2.5
Delamination $100\,\mathrm{mm}^2$	3.77
Surface layer	1.20

since any presence of a surface layer does not influence τ appreciably in this phase, and a clear difference between intact and delaminated tile can be identified. A difference of about 10 % between experimental data and FEM calculation is visible in Figure 4 and 5. The difference in the surface temperature can be explained by microscopic effects at the surface as described in the literature[33] while the difference in τ can result from the inhomogeneous thermal properties of the CFC.

IV. DISTRIBUTION OF DECAY TIME τ IN THE EXPERIMENTAL DATA

In a first step, archive data from HHF loading experiemnts at GLADIS (**G**arching **LA**rge **DI**vertor **S**ample Test Facility)[28] were used to verify the findings from the FEM calculations. In GLADIS, samples can be exposed to heat loads from $2\,MW/m^2$ to $55\,MW/m^2$ for pulse

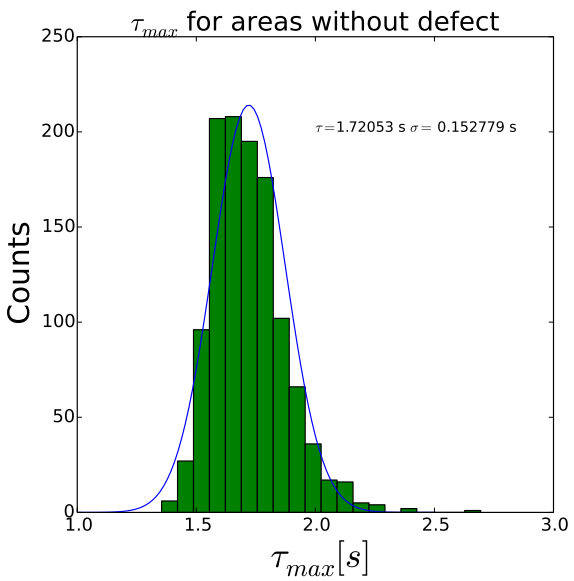

Figure 6: Distribution of τ_{max} for ROIs without known defects. Results from the qualification tests were used to sort out tiles with defects. $\tau_{mean} = 1.72\,\mathrm{s}$ with $\sigma = 0.15\,\mathrm{s}$

lengths of up to 30 s. The main mission of the device is to qualify and test plasma-facing components under realistic load conditions, and has been used extensively during the development and qualification of the W7-X HHF divertor elements. Two hydrogen neutral beams are available with a Gaussian heat flux profile of 100 mm mean width diameter at the target position. The target is observed by cameras operating in the visible and infrared range. A detailed description of the GLADIS facility and further available diagnostic can be found in[29]. The infrared archive data has a frame rate of 10 Hz and a spatial resolution of 1 mm/px. Observations were made in the wavelength range of 8 μm to 12 μm.

For the final qualification of the W7-X target elements, prototype elements were exposed to the heat flux of 10.5 MW/m^2 for 10 s. A thermal equilibrium is reached after 6 - 8 s,within the exposure time of typical 10 s. The inlet temperature of the cooling water was $\sim 20\,^{\circ}C$ with a velocity of 8 m/s and a static pressure of 1 MPa. Target tiles were loaded between 100 to 10.000 cycles. IR camera data are available for a number of these tests. We used these records to study the evolution of the surface temperature during the transient phases of cooling and heating, so as to gain statistics on intact tiles under high loads. On each target element, three regions of interest were defined, each of them covering about 1/3 of a tile: the first region covered the upper edge, the second one covers target's center, and the

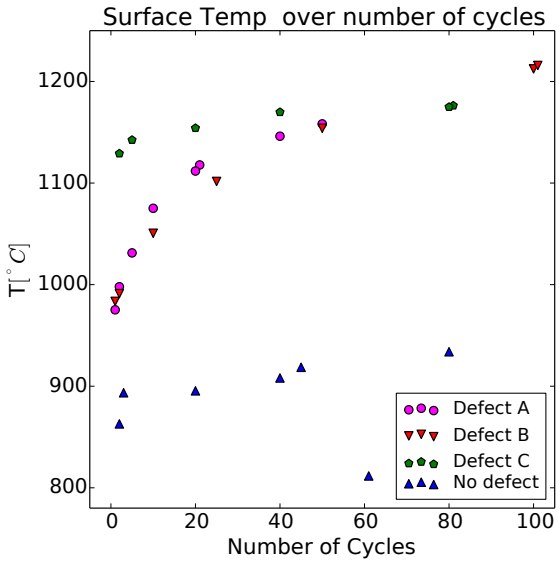

Figure 7: Steady state surface temperature for tiles exposed to a heat flux of $10.5\,MW/m^2$ (5% fluctuation). The surface temperature for non-defect tiles is in the range between $860\,°C$ and $1100\,°C$. An increase of the surface temperature is for all cases visible and two kinds of defects are visible: Fast-growing (Defect A and B), and slowly-growing (Defect C).

last one the lower edge. For each pixel τ was calculated after smoothing the temperature curves. A Blackman window[32] with a width of 5 frames was used. To further reduce the noise τ was averaged over three frames:

$$\tau = \frac{\tau_{i-1} + \tau_i(t \approx 10.5\,\mathrm{s}) + \tau_{i+1}}{3} \tag{2}$$

Here i denotes the frame number. For each region of interest the highest value of τ was taken. The resulting distribution of τ_{max} for all regions of interest with no known error is shown in figure 6. The mean value of this distribution is $\tau_{mean} = 1.72\,\mathrm{s}$ with $\sigma = 0.15\,\mathrm{s}$. For three known defects τ also was determined and compared to τ_{mean}. This error develop different over the number of heat cycles and is discussed in the following.

In figure 7 the local surface temperature for the three defects and for one tile with no defect are shown. When a target tile is loaded with $10.5\,MW/m^2$ the surface temperature typically varies between $860\,°C$ and $1100\,°C$[28] due to the scatter of CFC material properties[33,35]. From the evolution of the surface temperature two different behaviours for the defects can be deduced. Defect A and B show for their first recording a surface temperature within the range of an intact tile. For the following heat cycles the surface temperature increases

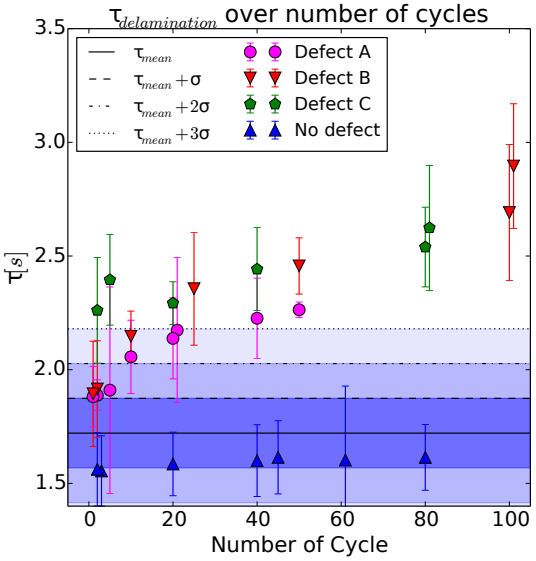

Figure 8: Decay time τ_{delam} for known defects. The growth of the delaminated areas is represented in the increase of τ_{delam} over the number of heat cycles.

rapidly until approximately 30 heat cycles ($\Delta T|_{1to30} = 130\,\mathrm{K}$) and increases slowly after wards ($\Delta T|_{30to100} = 90\,\mathrm{K}$). Defect C shows a surface temperature beyond $1100\,°C$ from the beginning and a slow but constant temperature increase for the following heat cycles ($\Delta T|_{1to80} = 30\,\mathrm{K}$). For the same cases the decay-times τ_{delam} are shown in figure 8. The distribution of decay-times for tiles without defects is shown in the background of the figure. Case A,B and C show a growing decay-time with the number of cycles. Also the decay-time trend shows a good agreement with the trend for the surface temperatures. τ_{delam} is increasing with the number of heat cycles, while the defects show the strongest growth of τ_{delam}.

We can distinguish between two types of defects: For defect C the interface was damaged from the beginning, which could be a production error. This defect is growing slow. Defects A and B are examples of the second type: these show an accelerating growth of the defect for the first heat cycles and a steady but sustained growth in subsequent heat cycles. These rapidly growing defects are critical for the lifetime of the divertor. The number of heat cycles onto tiles with such defects must be reduced as much as possible in order to allow for a long life. It should be mentioned here, that we measured the growing defects in an early prototype phase only. These kind of errors does not occur for the manufactured HHF targets, due to the higher performance of the final interface design[31].

V. DETECTION OF TILE DEFECTS IN THE PRESENCE OF SURFACE LAYERS

To investigate if defective tiles are still detectable by the τ-criteria ($\tau_{delam} > \tau_{mean} + 3\sigma$) in the presence of surface layers, a prototype target element with artificial amorphous hydrocarbon (a-C:H) layers was tested at GLADIS. The most common mechanism of surface layer formation is the re-deposition of eroded material from the PFCs. In a hydrogen-isotope plasma device with carbon as the main PFM, surface layers consist mostly of a-C:H. Traces of metallic components can also be found in such surface layers[34], if metal (typically steel) components are also exposed directly or indirectly to the plasma.

The target element used for these experiment already were exposed to heat flux prior to our experiments at least a hundred times, straining the interface between CFC tile and heat sink. Several tiles have known and well-characterized defects errors which were documented during the qualification tests (see IV). To determine the influence of surface layers on detecting defective interfaces we first exposed the tiles without a surface layer to a heat flux of $8.5\,\mathrm{MW/m^2}$. These experiments were performed directly after the commissioning of GLADIS after a prolonged shut down, therefore the calibration of the ion sources changed resulting in the lower power density. The average τ was measured for the center, the top and lower edge of the tiles. Figure 9 *a* shows the decay times for the reference shots.

Four tiles were coated with a-C:H layers of different thickness ($1\,\mu m$,$2\,\mu m$, $4\,\mu m$, $8\,\mu m$) at IPP Garching. Afterwards they were exposed to a heat flux of $10.5\,MW/m^2$ for 10 s. For some tiles, the measured surface temperature rose for some tiles to values of $1600\,^{\circ}C$. The results for τ can be seen in figure 9 *b*.

In Figure 10 an overview of the tile state determined by our reference experiment and a comparison with the results from the GLADIS qualification tests is shown. During the qualification tests tile 3,4 and 7 were determined to likely be defect and tile 5 and 6 were classified defective. In our experiments tile 3 to 5 and 7 to 8 were classified as defective, while tile 6 showed only a slight increase in τ at the upper edge. Visual inspection of the interfaces[23] of the tiles revealed, that the interface of tile 6 shows only a small crack at the lower interface. This crack also is not continuous over the area which could explain the small increase of τ. Nevertheless the surface temperature of tile 6 is greater than 1100 °C,

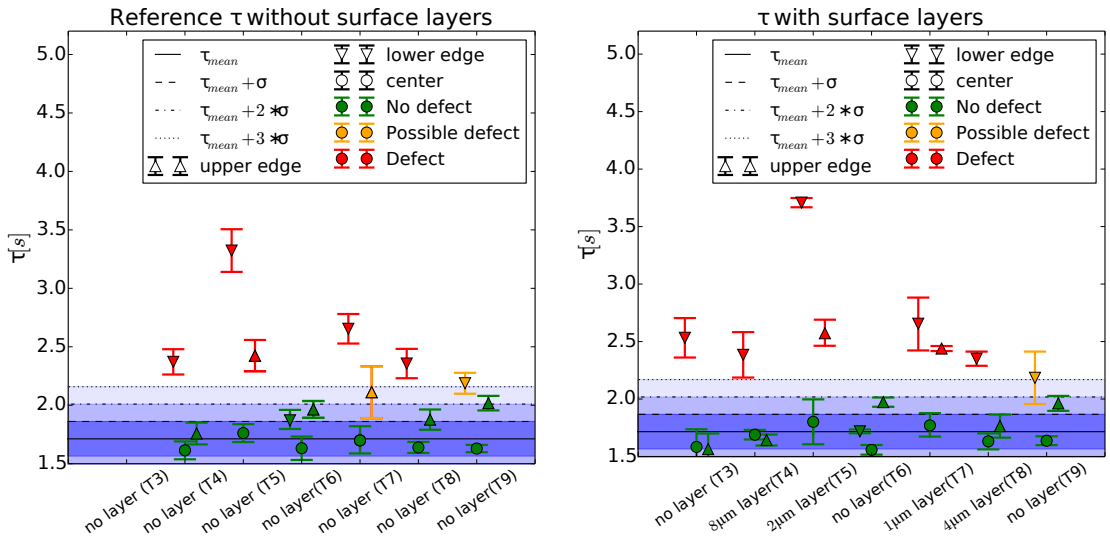

(a) No surface layer.

(b) With surface layer.

Figure 9: Decay times for known defects without (a) and with (b) surface layers. Notice that the presence of the surface layer does not hinder the detection of the defects. For the experiment without a surface layer no data for tile 3 is available.

which still is within the scatter of the CFC properties but higher than the allowed surface temperature. While the cause of the increased surface temperature needs to be further investigated it represents no threat to the safe operation of the machine.

The results do not change significantly when surface layers are added. The measured surface temperature rose for tile 8 ($4\,\mu m$ - layer) and some hot spots on tiles 5 and 4 up to $1600\,°C$. These hot spots are areas where the a-C:H layer is much thicker than anticipated. Nevertheless the results for τ show no significant deviation from the experiments with out surface layers (see figure 9).

VI. CONCLUSION AND OUTLOOK

It has been shown that it is possible to detect delamination defects, even in the presence of surface coatings, of CFC divertor tiles under plasma loading conditions, using the τ-criteria which is based solely on infrared camera measurements and can be calculated with relatively low computational effort. Thus, the structural health of the divertor tiles can be determined in situ, and essentially in real-time, by comparing the temperature decay time τ of a pixel

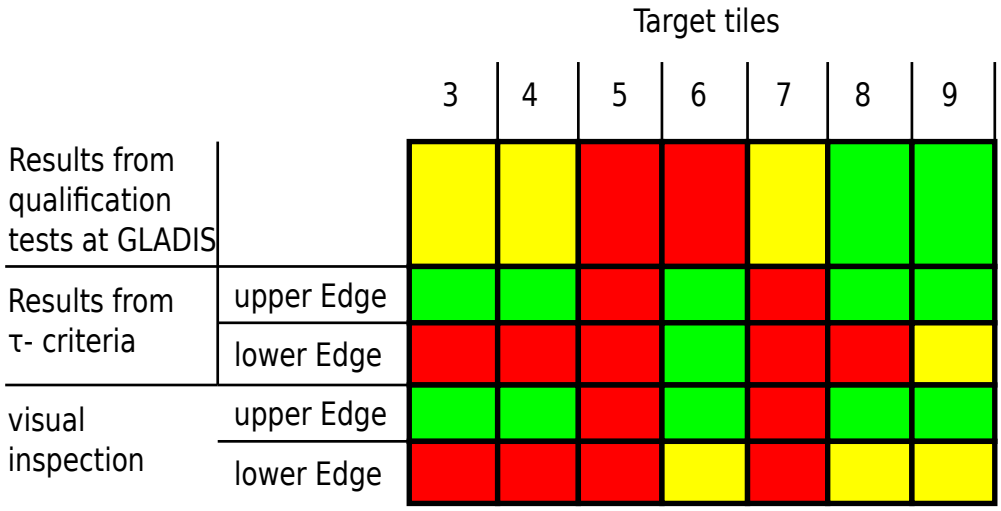

Figure 10: Overview of tile states found during the qualification tests, our experiments and visual inspection. Green indicates intact bonds, yellow are questionable, and red indicates defects. The visual inspection is in good agreement with our findings while there is a discrepancy between our experiments and the results from the qualification experiments. They are discussed in the text.

to the known distribution of τ for intact tiles. The criteria require a modulation in the local heat fluxes onto the components, in order to diagnose the health condition of divertor tiles during plasma operation. Therefore, plasma discharge scenarios must be developed that modulate the local divertor heat loads in a controlled way, without negatively affecting the plasma performance. The so-called control coils[26] are expected to be able to provide this modulation.

The criteria is already implemented in a fully automated computer algorithm that gives robust results. Future work is needed to implement the algorithm in a real-time system that has the needed response time. Also, the camera data used here have significantly higher spatial resolution (1 mm) than what will be available in W7-X (6-10 mm) and thus the minimum size of a delamination to be detectable will be greater then in the here presented experiments. Therefore, the effectiveness of the algorithm must be tested for a situation with a realistic spatial resolution and potentially developed further if the performance is significantly degraded as a result.

ACKNOWLEDGMENTS

This work has been carried out within the framework of the EUROfusion Consortium and has received funding from the European Union's Horizon 2020 research and innovation programme under grant agreement number 633053. The views and opinions expressed herein do not necessarily reflect those of the European Commission.

REFERENCES

[1]Andrew, P.; Coad, J.; Eich, T.; Gauthier, E.; Herrmann, A.; Matthews, G.; Riccardo, V. und Stamp, M. *Thermal effects of surface layers on divertor target plates.* Journal of Nuclear Materials, 313–316(0):135 – 139, 2003. ISSN 0022-3115. doi: http://dx.doi.org/10.1016/S0022-3115(02)01586-6. Plasma-Surface Interactions in Controlled Fusion Devices 15. 4

[2]Boscary, J.; Peacock, A.; Smirnow, M. und Tittes, H. *Summary of Research and Development Activities for the Production of the Divertor Target Elements of Wendelstein 7-X.* Plasma Science, IEEE Transactions on, 42(3):533–538, 2014. ISSN 0093-3813. doi: 10.1109/TPS.2014.2300195. 3, 13

[3]Boscary, J.; Stadler, R.; Peacock, A.; Hurd, F.; Vorköper, A.; Mendelevitch, B.; Cardella, A.; Pirsch, H.; Tittes, H.; Tretter, J.; Li, C.; Greuner, H. und Smirnow, M. *Design and technological solutions for the plasma facing components of WENDELSTEIN 7-X.* Fusion Engineering and Design, 86(6–8):572 – 575, 2011. ISSN 0920-3796. doi: 10.1016/j.fusengdes.2010.11.020. Proceedings of the 26th Symposium of Fusion Technology (SOFT-26). 2

[4]Cantarini, J.; Hildebrandt, D.; König, R.; Klinkhamer, F.; Moddemeijer, K.; Vliegenthart, W. und Wolf, R. *Optical design study of an infrared visible viewing system for Wendelstein 7-X divertor observation and controla).* Review of Scientific Instruments, 79(10):10F513, 2008. doi:http://dx.doi.org/10.1063/1.2979880. 3

[5]Füllenbach, F.; Rummel, T.; Pingel, S.; Laqua, H.; Müller, I. und Jauregi, E. *Final test of the W7-X control coils power supply and its integration into the overall control environment.* Fusion Engineering and Design, 82(5–14):1391 – 1395, 2007. ISSN 0920-3796. doi:http://dx.doi.org/10.1016/j.fusengdes.2007.03.052. Proceedings of the 24th Sympo-

sium on Fusion Technology SOFT-24. 15

[6]Gasparotto, M.; Baylard, C.; Bosch, H.-S.; Hartmann, D.; Klinger, T.; Vilbrandt, R. und Wegener, L. *Wendelstein 7-X—Status of the project and commissioning planning.* Fusion Engineering and Design, 89(9–10):2121 – 2127, 2014. ISSN 0920-3796. doi: http://dx.doi.org/10.1016/j.fusengdes.2014.02.075. Proceedings of the 11th International Symposium on Fusion Nuclear Technology-11 (ISFNT-11) Barcelona, Spain, 15-20 September, 2013. 2

[7]Greuner, H.; Boeswirth, B.; Boscary, J. und McNeely, P. *High heat flux facility GLADIS:: Operational characteristics and results of W7-X pre-series target tests.* Journal of Nuclear Materials, 367–370, Part B(0):1444 – 1448, 2007. ISSN 0022-3115. doi: 10.1016/j.jnucmat.2007.04.004. 9, 11

[8]Greuner, H.; Bolt, H.; Böswirth, B.; Franke, T.; McNeely, P.; Obermayer, S.; Rust, N. und Süß, R. *Design, performance and construction of a 2MW ion beam test facility for plasma facing components.* Fusion Engineering and Design, 75–79(0):345 – 350, 2005. ISSN 0920-3796. doi:http://dx.doi.org/10.1016/j.fusengdes.2005.06.021. Proceedings of the 23rd Symposium of Fusion Technology {SOFT} 23. 10

[9]Greuner, H.; Böswirth, B.; Boscary, J.; Chaudhuri, P.; Schlosser, J.; Friedrich, T.; Plankensteiner, A. und Tivey, R. *Cyclic heat load testing of improved CFC/Cu bonding for the W 7-X divertor targets.* Journal of Nuclear Materials, 386–388(0):772 – 775, 2009. ISSN 0022-3115. doi:10.1016/j.jnucmat.2008.12.214. 3

[10]Greuner, H.; Toussaint, U.; Böswirth, B.; Boscary, J.; Maier, H.; Peacock, A. und Traxler, H. *Performance and statistical quality assessment of {CFC} tile bonding on the pre-series elements of the Wendelstein 7-X divertor.* Fusion Engineering and Design, 86(9–11):1685 – 1688, 2011. ISSN 0920-3796. doi:http://dx.doi.org/10.1016/j.fusengdes.2010.12.025. Proceedings of the 26th Symposium of Fusion Technology (SOFT-26). 12

[11]Harris, F. *On the use of windows for harmonic analysis with the discrete Fourier transform.* Proceedings of the IEEE, 66(1):51–83, 1978. ISSN 0018-9219. doi: 10.1109/PROC.1978.10837. 11

[12]Herrmann, A. *Surface temperature measurement and heat load estimation for carbon targets with plasma contact and machine protection.* Physica Scripta, 2007(T128):234, 2007. 9, 11

[13]Hildebrandt, D.; Dübner, A.; Greuner, H. und Wiltner, A. *Thermal response to heat fluxes of the W7-AS divertor surface submitted to surface modification under high temperature treatment.* Journal of Nuclear Materials, 390–391(0):1118 – 1122, 2009. ISSN 0022-3115. doi:http://dx.doi.org/10.1016/j.jnucmat.2009.01.288. Proceedings of the 18th International Conference on Plasma-Surface Interactions in Controlled Fusion Device Proceedings of the 18th International Conference on Plasma-Surface Interactions in Controlled Fusion Device. 4, 13

[14]Hildebrandt, D.; Naujoks, D. und Sünder, D. *Surface temperature measurements of carbon materials in fusion devices.* Journal of Nuclear Materials, 337–339(0):1064 – 1068, 2005. ISSN 0022-3115. doi:http://dx.doi.org/10.1016/j.jnucmat.2004.09.033. PSI-16. 11

[15]Jacob, W. *Redeposition of hydrocarbon layers in fusion devices.* Journal of Nuclear Materials, 337–339(0):839 – 846, 2005. ISSN 0022-3115. doi: http://dx.doi.org/10.1016/j.jnucmat.2004.10.035. PSI-16. 4

[16]Jakubowski, M. W.; Biedermn, C.; König, R.; Lorenz, A.; Pedersen, T. S.; Rodatos, A. und team, W. .-X. *Development of infrared and visible endoscope as the safety diagnostic for steady- state operation of Wendelstein 7-X.* In *Conference QIRT 2014 (Bordeaux, France), 7-11 July 2014*, Bd. QIRT-2014-100. Conference QIRT 2014 (Bordeaux, France), 7-11 July 2014, 2014. 3

[17]König, R.; Hildebrandt, D.; Hübner, T.; Klinkhamer, F.; Moddemeijer, K. und Vliegenthart, W. *Optical design study for divertor observation at the stellarator W7-X.* Review of Scientific Instruments, 77(10):10F121, 2006. doi:http://dx.doi.org/10.1063/1.2220075. 3

[18]Martin, C.; Ruffe, R.; Pardanaud, C.; Cabié, M.; Dominici, C.; Dittmar, T.; Languille, P.; Pégourié, B.; Tsitrone, E. und Roubin, P. *Structure of the carbon layers deposited on the toroidal pump limiter of Tore Supra.* Journal of Nuclear Materials, 415(1, Supplement):S258 – S261, 2011. ISSN 0022-3115. doi: http://dx.doi.org/10.1016/j.jnucmat.2010.11.006. Proceedings of the 19th International Conference on Plasma-Surface Interactions in Controlled Fusion. 4

[19]Mitteau, M.; Vallet, J. C.; Reichle, R.; Brosset, C.; Chappius, P.; Cordier, J. J.; Delchambre, E.; Escourbiac, F.; Grosman, A.; Guilhem, D.; Lipa, M.; Loarer, T.; Schlosser, J. und Tsitrone, E. *Evolution of Carbon Tiles During Repetitive Long Pulse Operation in TORE SUPRA.* Physica Scripta, 2004(T111):157, 2004. 3, 8

[20]Peng, X.; Bykov, V.; Köppen, M.; Ye, M.; Fellinger, J.; Peacock, A.; Smirnow, M.; Boscary, J.; Tereshchenko, A. und Schauer, F. *Thermo-mechanical analysis of Wendelstein 7-X plasma facing components.* Fusion Engineering and Design, 88(9–10):1727 – 1730, 2013. ISSN 0920-3796. doi:http://dx.doi.org/10.1016/j.fusengdes.2013.03.056. Proceedings of the 27th Symposium On Fusion Technology (SOFT-27); Liège, Belgium, September 24-28, 2012. 7

[21]Pintsuk, G.; Compan, J.; Linke, J.; Majerus, P.; Peacock, A.; Pitzer, D. und Rödig, M. *Mechanical and thermo-physical characterization of the carbon fibre composite NB31.* Physica Scripta, 2007(T128):66, 2007. 2, 7

[22]Andrew, P.; Coad, J.; Eich, T.; Gauthier, E.; Herrmann, A.; Matthews, G.; Riccardo, V. und Stamp, M. *Thermal effects of surface layers on divertor target plates.* Journal of Nuclear Materials, 313–316(0):135 – 139, 2003. ISSN 0022-3115. doi: http://dx.doi.org/10.1016/S0022-3115(02)01586-6. Plasma-Surface Interactions in Controlled Fusion Devices 15. 4

[23]Boscary, J.; Peacock, A.; Smirnow, M. und Tittes, H. *Summary of Research and Development Activities for the Production of the Divertor Target Elements of Wendelstein 7-X.* Plasma Science, IEEE Transactions on, 42(3):533–538, 2014. ISSN 0093-3813. doi: 10.1109/TPS.2014.2300195. 3, 13

[24]Boscary, J.; Stadler, R.; Peacock, A.; Hurd, F.; Vorköper, A.; Mendelevitch, B.; Cardella, A.; Pirsch, H.; Tittes, H.; Tretter, J.; Li, C.; Greuner, H. und Smirnow, M. *Design and technological solutions for the plasma facing components of WENDELSTEIN 7-X.* Fusion Engineering and Design, 86(6–8):572 – 575, 2011. ISSN 0920-3796. doi: 10.1016/j.fusengdes.2010.11.020. Proceedings of the 26th Symposium of Fusion Technology (SOFT-26). 2

[25]Cantarini, J.; Hildebrandt, D.; König, R.; Klinkhamer, F.; Moddemeijer, K.; Vliegenthart, W. und Wolf, R. *Optical design study of an infrared visible viewing system for Wendelstein 7-X divertor observation and controla).* Review of Scientific Instruments, 79(10):10F513, 2008. doi:http://dx.doi.org/10.1063/1.2979880. 3

[26]Füllenbach, F.; Rummel, T.; Pingel, S.; Laqua, H.; Müller, I. und Jauregi, E. *Final test of the W7-X control coils power supply and its integration into the overall control environment.* Fusion Engineering and Design, 82(5–14):1391 – 1395, 2007. ISSN 0920-3796. doi:http://dx.doi.org/10.1016/j.fusengdes.2007.03.052. Proceedings of the 24th Sympo-

sium on Fusion Technology SOFT-24. 15

[27]Gasparotto, M.; Baylard, C.; Bosch, H.-S.; Hartmann, D.; Klinger, T.; Vilbrandt, R. und Wegener, L. *Wendelstein 7-X—Status of the project and commissioning planning.* Fusion Engineering and Design, 89(9–10):2121 – 2127, 2014. ISSN 0920-3796. doi: http://dx.doi.org/10.1016/j.fusengdes.2014.02.075. Proceedings of the 11th International Symposium on Fusion Nuclear Technology-11 (ISFNT-11) Barcelona, Spain, 15-20 September, 2013. 2

[28]Greuner, H.; Boeswirth, B.; Boscary, J. und McNeely, P. *High heat flux facility GLADIS:: Operational characteristics and results of W7-X pre-series target tests.* Journal of Nuclear Materials, 367–370, Part B(0):1444 – 1448, 2007. ISSN 0022-3115. doi: 10.1016/j.jnucmat.2007.04.004. 9, 11

[29]Greuner, H.; Bolt, H.; Böswirth, B.; Franke, T.; McNeely, P.; Obermayer, S.; Rust, N. und Süß, R. *Design, performance and construction of a 2MW ion beam test facility for plasma facing components.* Fusion Engineering and Design, 75–79(0):345 – 350, 2005. ISSN 0920-3796. doi:http://dx.doi.org/10.1016/j.fusengdes.2005.06.021. Proceedings of the 23rd Symposium of Fusion Technology {SOFT} 23. 10

[30]Greuner, H.; Böswirth, B.; Boscary, J.; Chaudhuri, P.; Schlosser, J.; Friedrich, T.; Plankensteiner, A. und Tivey, R. *Cyclic heat load testing of improved CFC/Cu bonding for the W 7-X divertor targets.* Journal of Nuclear Materials, 386–388(0):772 – 775, 2009. ISSN 0022-3115. doi:10.1016/j.jnucmat.2008.12.214. 3

[31]Greuner, H.; Toussaint, U.; Böswirth, B.; Boscary, J.; Maier, H.; Peacock, A. und Traxler, H. *Performance and statistical quality assessment of {CFC} tile bonding on the pre-series elements of the Wendelstein 7-X divertor.* Fusion Engineering and Design, 86(9–11):1685 – 1688, 2011. ISSN 0920-3796. doi:http://dx.doi.org/10.1016/j.fusengdes.2010.12.025. Proceedings of the 26th Symposium of Fusion Technology (SOFT-26). 12

[32]Harris, F. *On the use of windows for harmonic analysis with the discrete Fourier transform.* Proceedings of the IEEE, 66(1):51–83, 1978. ISSN 0018-9219. doi: 10.1109/PROC.1978.10837. 11

[33]Herrmann, A. *Surface temperature measurement and heat load estimation for carbon targets with plasma contact and machine protection.* Physica Scripta, 2007(T128):234, 2007. 9, 11

[34]Hildebrandt, D.; Dübner, A.; Greuner, H. und Wiltner, A. *Thermal response to heat fluxes of the W7-AS divertor surface submitted to surface modification under high temperature treatment.* Journal of Nuclear Materials, 390–391(0):1118 – 1122, 2009. ISSN 0022-3115. doi:http://dx.doi.org/10.1016/j.jnucmat.2009.01.288. Proceedings of the 18th International Conference on Plasma-Surface Interactions in Controlled Fusion Device Proceedings of the 18th International Conference on Plasma-Surface Interactions in Controlled Fusion Device. 4, 13

[35]Hildebrandt, D.; Naujoks, D. und Sünder, D. *Surface temperature measurements of carbon materials in fusion devices.* Journal of Nuclear Materials, 337–339(0):1064 – 1068, 2005. ISSN 0022-3115. doi:http://dx.doi.org/10.1016/j.jnucmat.2004.09.033. PSI-16. 11

[36]Jacob, W. *Redeposition of hydrocarbon layers in fusion devices.* Journal of Nuclear Materials, 337–339(0):839 – 846, 2005. ISSN 0022-3115. doi: http://dx.doi.org/10.1016/j.jnucmat.2004.10.035. PSI-16. 4

[37]Jakubowski, M. W.; Biedermn, C.; König, R.; Lorenz, A.; Pedersen, T. S.; Rodatos, A. und team, W. .-X. *Development of infrared and visible endoscope as the safety diagnostic for steady- state operation of Wendelstein 7-X.* In *Conference QIRT 2014 (Bordeaux, France), 7-11 July 2014*, Bd. QIRT-2014-100. Conference QIRT 2014 (Bordeaux, France), 7-11 July 2014, 2014. 3

[38]König, R.; Hildebrandt, D.; Hübner, T.; Klinkhamer, F.; Moddemeijer, K. und Vliegenthart, W. *Optical design study for divertor observation at the stellarator W7-X.* Review of Scientific Instruments, 77(10):10F121, 2006. doi:http://dx.doi.org/10.1063/1.2220075. 3

[39]Martin, C.; Ruffe, R.; Pardanaud, C.; Cabié, M.; Dominici, C.; Dittmar, T.; Languille, P.; Pégourié, B.; Tsitrone, E. und Roubin, P. *Structure of the carbon layers deposited on the toroidal pump limiter of Tore Supra.* Journal of Nuclear Materials, 415(1, Supplement):S258 – S261, 2011. ISSN 0022-3115. doi: http://dx.doi.org/10.1016/j.jnucmat.2010.11.006. Proceedings of the 19th International Conference on Plasma-Surface Interactions in Controlled Fusion. 4

[40]Mitteau, M.; Vallet, J. C.; Reichle, R.; Brosset, C.; Chappius, P.; Cordier, J. J.; Delchambre, E.; Escourbiac, F.; Grosman, A.; Guilhem, D.; Lipa, M.; Loarer, T.; Schlosser, J. und Tsitrone, E. *Evolution of Carbon Tiles During Repetitive Long Pulse Operation in TORE SUPRA.* Physica Scripta, 2004(T111):157, 2004. 3, 8

[41]Peng, X.; Bykov, V.; Köppen, M.; Ye, M.; Fellinger, J.; Peacock, A.; Smirnow, M.; Boscary, J.; Tereshchenko, A. und Schauer, F. *Thermo-mechanical analysis of Wendelstein 7-X plasma facing components.* Fusion Engineering and Design, 88(9–10):1727 – 1730, 2013. ISSN 0920-3796. doi:http://dx.doi.org/10.1016/j.fusengdes.2013.03.056. Proceedings of the 27th Symposium On Fusion Technology (SOFT-27); Liège, Belgium, September 24-28, 2012. 7

[42]Pintsuk, G.; Compan, J.; Linke, J.; Majerus, P.; Peacock, A.; Pitzer, D. und Rödig, M. *Mechanical and thermo-physical characterization of the carbon fibre composite NB31.* Physica Scripta, 2007(T128):66, 2007. 2, 7